A New Dorsal Hand Vein Authentication System Based on Fractal Dimension Box Counting Method

MURAT ERHAN CIMEN,[1,*] OMER FARUK BOYRAZ,[1] MUSTAFA ZAHID YILDIZ[1] AND ALI FUAT BOZ[1]

[1]Electrical and Electronic Engineering Department, Sakarya University of Applied Sciences, Serdivan, Sakarya, 54050 TURKEY
*muratcimen@subu.edu.tr

Abstract:

Dorsal hand vein pattern is a physiological feature that can distinguish and define one person from another. Feature extraction from images is considered as the most important step in biometric systems. In this study, a fractal technique, which is both an advanced and a complex method, is proposed for feature extraction from the images of hand vessel pattern. In recent years, this approach has been widely used as an active research area in image processing. Therefore, fractal size based tissue analysis method, which is calculated by box counting method, which is a new technique in determining the tissue properties of the dorsal hand vein, has been applied. Experimental findings on the dorsal vein databases of Bosphorous and SUAS show that our proposed method yields promising and optimistic results compared to other known techniques.

Keyword. Fractal dimension, box counting, hand vein recognition

1. Introduction

Biometry allows people to be differentiated according to their specific physiological and behavioral attributes, such as iris, fingerprint, shape of the face and patterns of motion. Physiological characteristics such as fingerprints, facial characteristics are related to body shape, while behavioral characteristics such as signature, voice tone and speech styles are related to the person's behavioral pattern. It is extremely difficult to change the vascular pattern under the skin surgically. For this reason, it is extremely reliable to use an identification system created using dorsal hand vein patterns that are unique for person in biometric systems. Vein patterns are hidden under the skin and difficult to obtained or scanned under visible light, making it advantageous to use in authentication applications [1]. An advantage of performing authentication from hand vein patterns compared to other pattern recognition systems (such as fingerprints, palm prints, finger veins) is that they can be processed in a contactless manner during identification and authentication [2]. In this way, identification is done in a more sterile environment. Authentication systems made by contact with a platform can be done incorrectly due to contamination of the contacted surface (sweating, wetness, scratching of the surface etc.). Commonly in the literature, vein recognition technologies include the following steps, respectively; image acquisition, pre-processing of the vein images, feature extraction and recognition from the vein images. Most of the recommended methods for attribute extraction are for local and global texture features extracted from vein images to determine the properties of the vein model. In their study, Li et al. transformed the images of hand veins into 1 bit by passing them through various image processing algorithms. Then, they extracted 7 Hu moments (translation, rotation and scale invariant) from the segmented images. These feature vectors

were entered into SVM for training and testing. As a result of the experiment, they reached 95.5% accuracy rate [3]. Wang et al. developed a person verification system from hand vein patterns using thermal imaging technique. They proposed a vessel matching procedure based on the line segment Hausdorff distance (LHD). They found that all subjects were correctly recognized in their trials on 30-person thermal vein images [4]. Khan et al. after collecting the hand vein images with a low cost CCD camera, they segmented the vein areas. Principle Component Analysis (PCA) method, which is successful in recognizing human faces, has been applied to vascular images. Low-dimensional eigenvalues were obtained from the vessel pattern using the PCA method. The developed system has been successfully tested on a 200 image database [5]. Biometric Graph Matching (BGM) algorithm, one of the other global features extraction methods, was proposed by Lajevardi et al. Two different cost functions have been developed for BGM and compared to iterative closest point (ICP) and Modified hausdorf distance (MHD) algorithms, which are standard point pattern mappings [6]. Other algorithms used to extract features from vessel images are local feature-based methods. Local feature-based methods such as Scale Invariant Feature transfor (SIFT), Speeded Up Robust Feature (SURF), Binary Robust invariant scalable keypoints (BRISK), Fast Retina Keypoint (FREAK) detect local key points on pixels, therefore compared to global feature-based methods they are more durable. Wang et al. have developed an identification system from dorsal hand vein images. The images are segmented after various improvement algorithms. After the segmentation, local key points were extracted from the vein images using the SIFT algorithm. As a result of the studies carried out on a dataset with more than 2000 vein images, it has been observed that the system's recognition rate has reached 100% [7]. In another study, Huang et al. Proposed a new authentication approach using NCUT (North China University of Tech.) Handheld vein images. In the proposed method, they developed a new shape representation method to define the geometric structure of vascular networks with a local and holistic approach. Local binary pattern (LBP) algorithm was used for feature extraction and extensive experiments were done on NCUT. According to the experimental results performed with the proposed method, the authentication success rate was found to be 99.21% [8].

In previous studies on hand vein recognition systems in the literature, it has been found that removing local invariant features is more suitable for contactless recognition. Local invariants are not affected by changes such as rotation, scale and depth.

In this study, a new approach was proposed to analyze the on-hand vein pattern using the fractal technique, and the box counting (BC) method, which provides a definition of the geometric properties of the image tissue, was used to estimate the fractal size. Firstly, unrelated areas of the image must be removed in order to speed up image processing and extract fractal dimension from the right regions. After extract the region of interest (ROI), the image is converted to gray level, contrast-limited adaptive histogram equalization, median filtering, adaptive thresholding and morphological processes are applied, and segmentation of vein patterns is provided. After segmentation, fractal dimensions of 1-bit images were calculated by BC method. In order to reduce the effect of the image from the turning angles, a circle area has been determined based on the center of the selected region of interest. In this way, the fractal dimensions can be calculated by rotating the image around this center at certain angles. Fractal size calculation was made for each angle by rotating this selected area around the center point at intervals of 10 degrees from -30 degrees to 30 degrees. Then fractal dimension values calculated for a single vein pattern are stored in the database as feature vectors. Finally, dorsal hand vein recognition was performed by KNN, SVM classifiers with different parameters.

The effectiveness of fractal dimensions in analyzing the image of on-hand vein pattern, Bosphorous hand vein and SUAS (Sakarya University of Applied Sciences) hand vein database [9] were evaluated. Unlike most related studies using a small database, our studies have been performed on larger databases that may contain variability in lighting conditions and tissue deformation between images. Fractal dimensions calculated from segmented vessel patterns are

trained and tested in classification models such as SVM and KNN. 100% performance rate has been achieved with the SVM classification algorithm on the SUAS database.

2. Materials and methods

2.1 Data collection procedure and creating the database

In this study, near infrared imaging technology was used to obtain vein images. The left and right surfaces of the subjects hands were illuminated with two 850nm wavelength infrared power leds. The Kodak 87C filter is installed in front of the camera lens to prevent visible light from reaching the infrared camera and to filter out various ambient noises. The lighting was kept constant throughout the experiment of the LED system's current supply.

The SUAS hand vein image database used in the study consists of 919 images taken from 155 healthy adults. None of them had any vascular surgery or other medical condition that could affect the results of the proposed method. Subjects were asked to bring their right and left hands to the fist position before taking images. Then they placed their fists flat on the green square area as in Fig. 1 In this way, hand vein images were taken from the subjects within 3 seconds. The procedures applied did not harm the participants.

Fig. 1. The procedure for creating the SUAS dorsal hand vein database

2.2 Methods

The flow diagram of the fractal dimension based vein identification system is shown in Fig. 2. After the hand vein raw image was taken with the infrared camera module, these images were processed using the open source Open-CV image processing library in the Phyton programming language. From the images taken, the region of interest are subtracted to shorten the processing time and calculate the fractal size only on the region of the vein pattern. Then, vein pattern was revealed by passing through gray level transformation, contrast limited adaptive histogram

equalization, median filtering, adaptive thresholding and morphological processes (opening, closing and erosion) [10]. After the image processing steps, the feature was extracted with the fractal size-based box counting method on the processed images, and the attribute information was obtained and this information was recorded in the database. In the verification step, the real-time handheld image taken by the infrared camera was passed through the image processing steps again and the fractal size was calculated on the processed image. Then, matching was made with the fractal size information in the database.

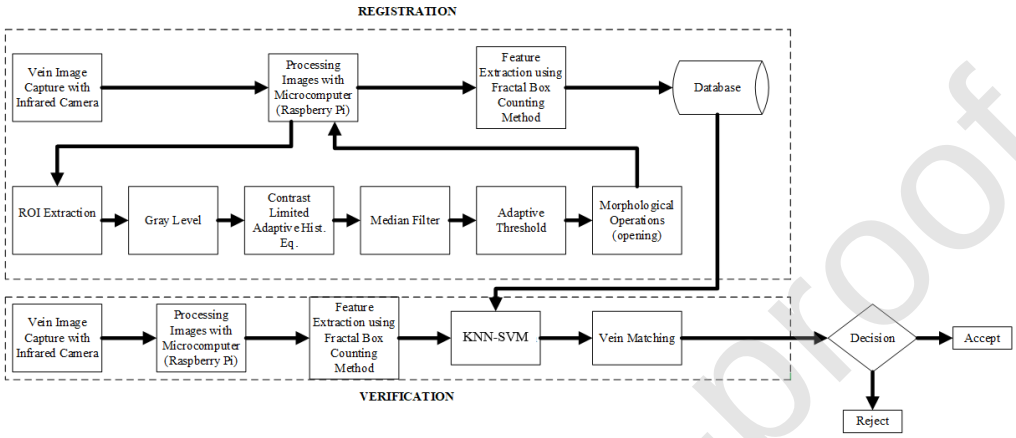

Fig. 2. Fractal Size based identification system general flow diagram

2.2.1 Normalizing images using the SURF method

The SURF (Speed Up Robust Feature) algorithm was developed by Herbert Bay in 2006 to determine local feature points, independent of rotation, scaling and translation in an image [11].

In this study, all images in the database were normalized and brought to the same position with the SURF method. In this way, the data received at different times or at different angles and scales were brought to the same position and the region of interests (ROI) were extracted (Fig. 3).

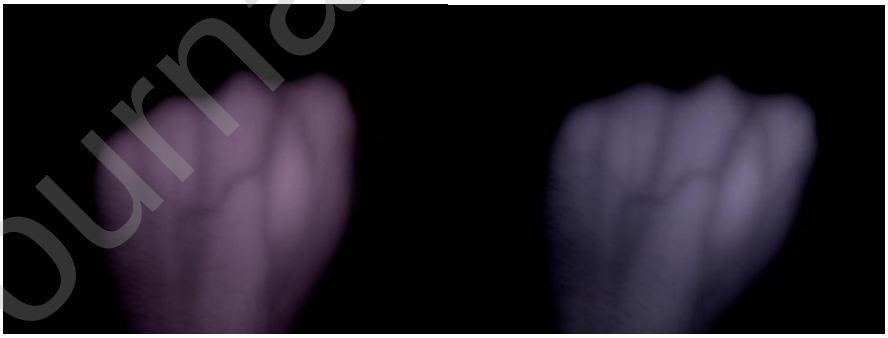

(a) (b)

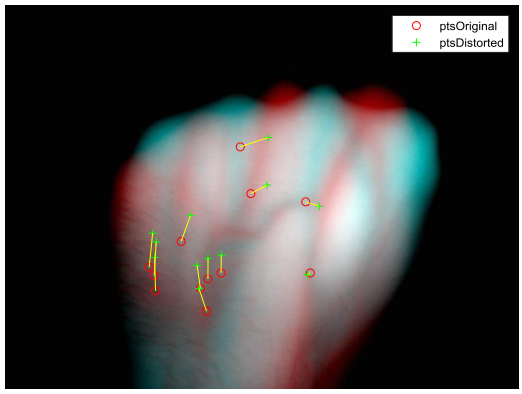

(c)

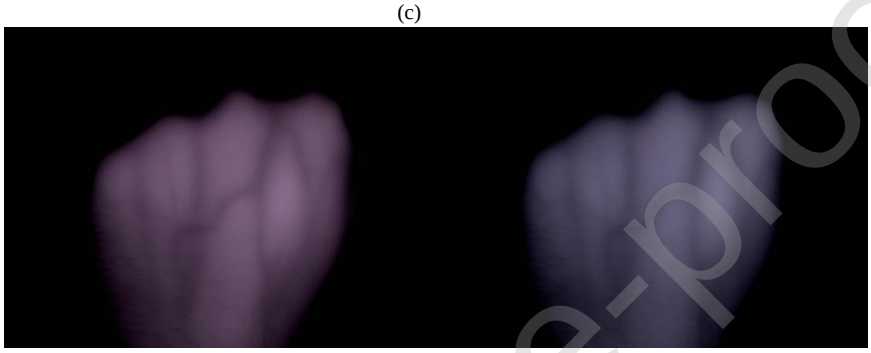

(d)

Fig. 3. a) Reference image of the 21rd person in the database b) Image of the same person taken at different angles and at different times c) Matching points (inliers only) d) Hand vein image was normalized to its reference images

2.2.2 Extracting the region of interest (ROI)

In order to accelerate the processing time and standardize the collection of vein images, Fig. 4 (a) was masked on the raw image taken and the borders of the hand surface area were determined. Then, the entire image was scanned from right to left and from top to bottom, pixel by pixel, and the first point that passed to the value of 255 pixels was found to be the tip of the bone indicated by the blue dot in Fig. 4 (b). Then, experimentally, a 256x256 pixel square region, which was selected below this point, went down to 150 pixels in Fig. 4 (c) and determined as the relevant target region (Fig. 4 (d)).

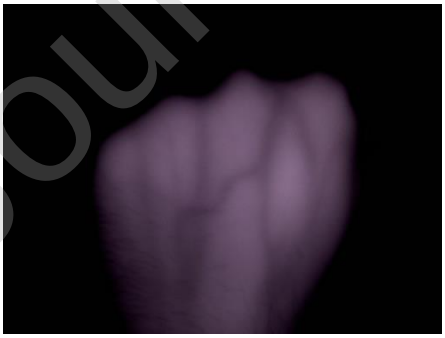

(a)

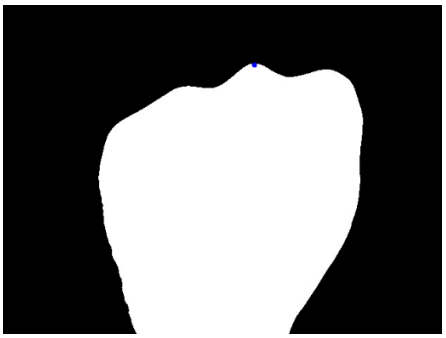

(b)

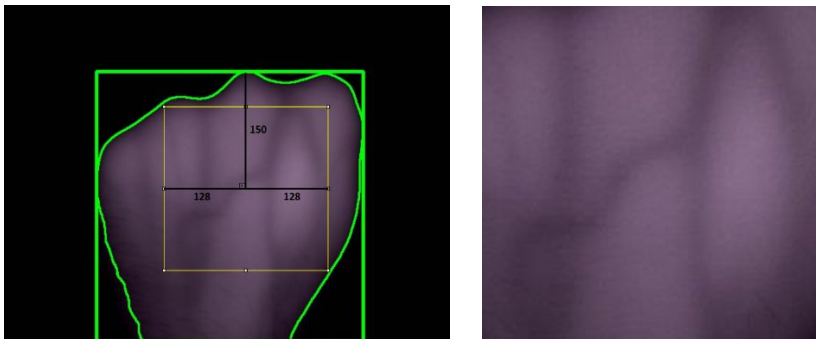

(c) (d)

Fig. 4 (a) Reference image of the 21rd person in the database (b) Segmentation of the hand image (c) Finding the Boundaries and Squareing the Hand Surface (d) Extracting the region of interest 256x256 pixels

2.2.3 Processing of dorsal hand vein images

The extracted target region is given in fig. 5 (a). Segmentation of the vascular structures was achieved by applying various image processing steps on the extracted target region. As a result of this process, fig. 5 (d) was obtained. After this operation, a circular region was removed to prevent the image from being affected by any possible rotation. For this, RIO has been converted to the figure in fig. 5 (e).

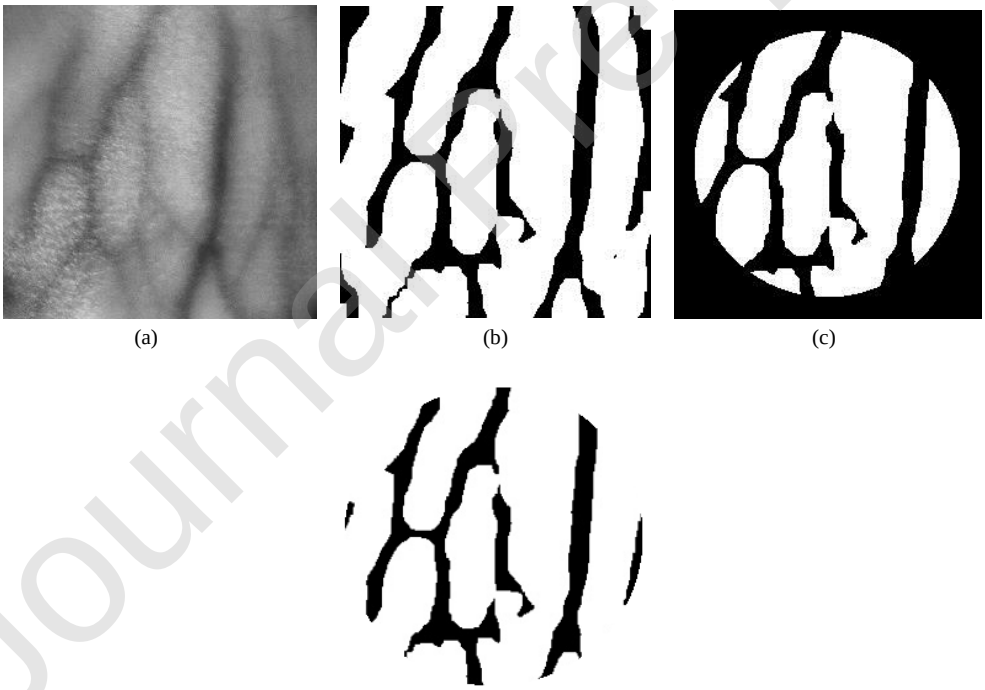

(a) (b) (c)

(d)

Fig. 5 (a) Obtained target region, (b) Processing the target region, (c) Extracting a circular section from the target region (d) Transforming the black region outside the circle to white (To prevent the change of the fractal dimension value)

3.2.4 Feature extraction with fractal size based box counting method

Fractal dimension calculation can be explained as the examination of the development of the proportions of details in different scales, existing in nature or in a designed structure. As the shape's value of fractal dimension increases, so does the details [12, 13]. As the fractal dimension found approaches 1, it shows that it approaches euclidean geometry and that the structure is not fractal. In other words, the larger the fractal dimension, the greater the specifics develop at different scales [12, 14-16]. The fractal dimension thus emerges as a function in the image. Methods of curling and box counting are used for calculating the fractal dimension in the image Curling method is a probability-based iterative process, as it is made using coins [17]. The method in itself continues until the process is balanced. On the other hand, box counting method is an iterative method for counting filled boxes that covers shape in the image at different scales [18, 19].

In the first iteration the image is divided into parts, counting the filled boxes on it. Then in the 2nd iteration, the picture is divided again, counting the number of boxes filled in. Fractal dimensions are calculated by using Equation (1) or (2). Generally, the values obtained as a result of the numbers of filled and empty boxes that appear with the grid formed as a result of each cycle are used in the calculation of the fractal dimension value [13, 20, 21]. Thus, fractal dimension values are found with the box counting method at the end of each cycle. This process continues until the fractal dimension value converges to a certain value. Fractal dimension values provide a relation between knowledge richness (depth and detail) and fractal continuity. The detail and richness of the image with a high fractal dimension value is also high [18, 19, 22]. To calculate fractal dimension using box counting method, Equation (1) is used. In this Equation (1), at the previous and present iterations, requires both number of filled boxes and sum of empty and filled number of boxes. Also Equation (1) can be expressed with Equation (2).

$$D = \frac{\log\left(\begin{matrix}\textit{filled boxes at}\\ \textit{present iteration}\end{matrix}\right) - \log\left(\begin{matrix}\textit{filled boxes at}\\ \textit{previos iteration}\end{matrix}\right)}{\log\left(\begin{matrix}\textit{sum of empty and}\\ \textit{filled boxes at}\\ \textit{present iteration}\end{matrix}\right) - \log\left(\begin{matrix}\textit{sum of empty and}\\ \textit{filled boxes at}\\ \textit{previos iteration}\end{matrix}\right)} \tag{1}$$

$$D_{i+1,i} = \frac{\log\left(N_{i+1}\right) - \log\left(N_i\right)}{\log\left(2^{i+1}\right) - \log\left(2^i\right)} \tag{2}$$

The vein image taken is given in Fig. 6 (a). In order to apply the box counting technique to the received image, the image is divided into boxes. This process is clearly given in Fig. 6. The image is divided into four equal parts in the 1st cycle. In the divided pieces, the part of the boxes that is fully filled is zero. Then the number of filled boxes was 4 in the first iteration. At 2nd iteration number of filled boxes was 13 and so on. Gray pixel values of the grids created on the images given in Fig. 6 are not included in the box counting operations software. Box counting method applied on the image is performed iteratively. The number of full-empty boxes formed as a result of 8 cycles is shown in Fig. 7. As can be seen in the figure, as the size of the boxes in the image gets smaller, the number of filled boxes on the image increases. The number of boxes obtained as a result of the iterations are given in Table 1.

Equation (2) is used to calculate the fractal dimension on the image. While doing this, the number of filled boxes obtained in each cycle was counted. The fractal dimension values calculated for the sample image are shown in Equation (3). The fractal richness of the image

was high as the fractal dimension was close to 2. The result obtained showed that the vein pattern is in fractal structure.

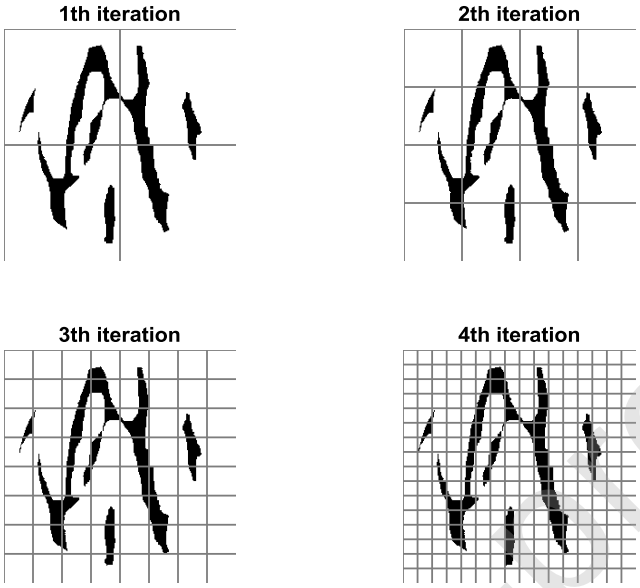

Fig. 6. (a) 1st iteration vein image, (b) 2nd iteration vein image, (c) 3rd iteration vein image (d) 4th iteration vein image

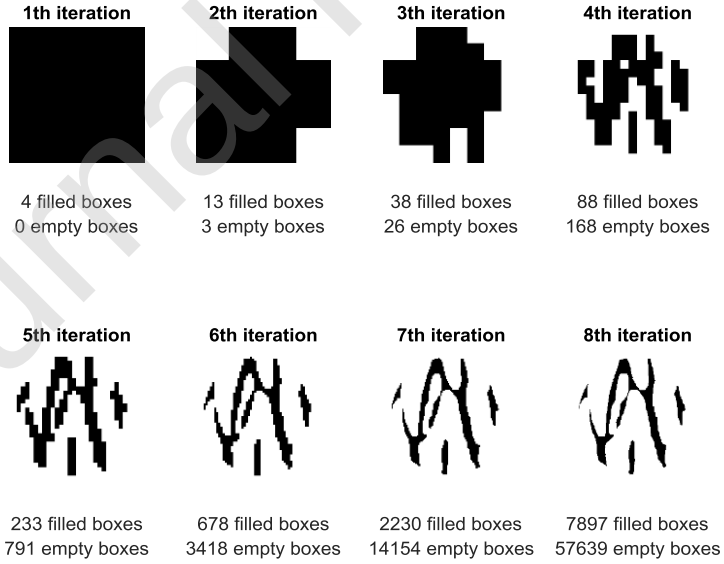

Fig. 7. Application of the box counting technique to the image

Table 1. Number of filled and empty boxes of each image of the boxes in the vein image.

	Filled Boxes	Empty Boxes
1 th iteration	4	0
2 nd iteration	13	3
3 th iteration	38	26
4 th iteration	88	168
5 th iteration	233	791
6 th iteration	678	3418
7 th iteration	2230	14154
8 th iteration	7897	57639

$$
\begin{aligned}
D_{1,2} &= \frac{\log(13)-\log(4)}{\log(4)-\log(2)} \\
D_{2,3} &= \frac{\log(38)-\log(13)}{\log(8)-\log(4)} \\
D_{3,4} &= \frac{\log(88)-\log(38)}{\log(16)-\log(8)} \\
D_{4,5} &= \frac{\log(233)-\log(88)}{\log(32)-\log(16)} \\
D_{5,6} &= \frac{\log(678)-\log(233)}{\log(64)-\log(32)} \\
D_{5,6} &= \frac{\log(2230)-\log(678)}{\log(128)-\log(64)} \\
D_{6,7} &= \frac{\log(7897)-\log(2230)}{\log(256)-\log(128)}
\end{aligned}
\tag{3}
$$

The pseudo code in Fig. 8 is given to demonstrate the applicability of the box counting technique used in the calculation of the fractal dimension to the image. The first command is run in this code. Then the image is taken on the 2nd line. In the 3th line, the size of the image taken is determined. In the 4th line, the number of parts that the image will be divided is determined. The aim of the 5-7th lines is to increase the image size if the number of boxes generated in the divided image isn't an integer. The number of divisions and the size in the image provides the value called the Least Common Multiple (LCM). On the 8th line, the size of the image is changed to LCM value and the size of the image is changed. In 9th line, the image is converted to binary image. A loop was created to find the boxes on the image in 10-11th lines. In the 12th line, the box on the image (i, j). the number of pixel values of the box has been found. In the 13-15th lines, if the entire box matches with the pixels of the vein pattern pixel, the variable value called "filledbox" number is increased, and the number of boxes in the image is found.

```
1 Start
2 I=import(image);
3 dimension=size(I);
4 number of segmentation is determined
```

```
5 while (box size is not an integer?)
6     dimension = dimension +1;
7 end while
8 image=imresize(I, dimension);
9 image to binary
10 for i=1: dimension / number of segmentation : dimension
11    for j=1: dimension / number of segmentation: dimension
12       pixel number= Find the number of black pixel between (i)th column (j)th line and
(i+1)th column (j+1)th Line in the image
13       if (is the number of pixels equal to the box size?)
14       filledbox = filledbox +1
15       end if
16   end for
17 end for
```

Fig. 8. Pseudo code of the box counting technique

The last fractal size value of the image is determined as a feature. An area has been chosen that will be rotated around the center of the image to reduce effects of the angles of turn. In this way, the fractal dimensions can be calculated by rotating the image around this center at certain angles. Figure 2.9 can be given for this. ROI is determined on the origanal image center. Then, the fractal dimension is calculated around this center, starting from -30 degrees to 30 degrees at intervals of 10 degrees. It has been given at 10 degree intervals to better transfer the images to the Fig. 9. But in practice, fractal dimensions were calculated with 5 degrees intervals and data were created. Also, to identify the person from the vein image, the fractal dimensions of the vein images taken on different subjects in Fig. 10 were calculated.

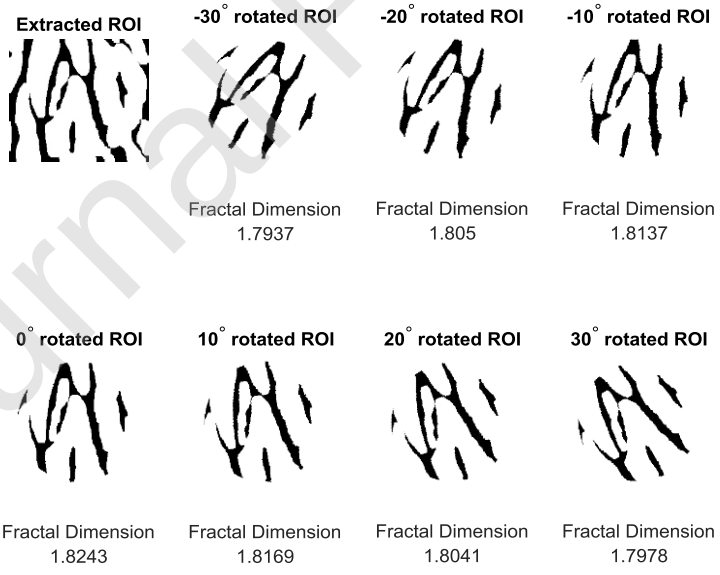

Fig. 9. Fractal dimensions of the vein image at different rotation angles

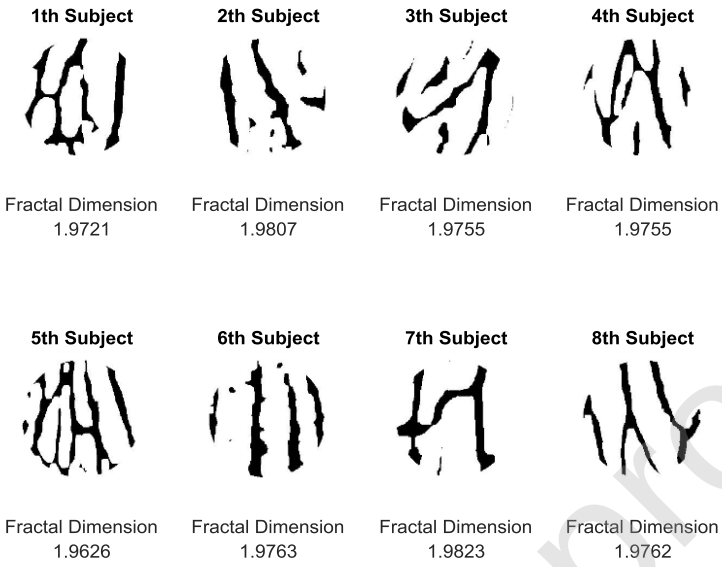

Fig. 10. Fractal dimensions of the vein image taken from different subjects

3.2.5 Knn algorithm

The main purpose in classification is to determine which class the objects belong to by looking at the properties of the objects [23, 24]. There are many methods for this process such as decision trees, nearest neighbor, artificial neural networks, fuzzy logic [24, 25]. The closest neighbor algorithm is a method used for both classification and regression. Basically, the distance of the new point in the data to the nearest points in the data is examined. K represents the number of the closest neighbors of the unknown point [23, 24, 26-28]. The k value is usually selected as an odd number to prevent uncertainty. The result obtained in Knn classification gives class membership in the dataset of the sample data. In KNN regression, k is the average of the values of k close neighbors of the new data. In other words, it represents the property value of the new data. The distance between the data can be calculated during the processing of the Knn algorithm using Euclidean function in Equation (4), Manhattan function in Equation (5) or Minkowski formulae in Equation (6). Generally, normalization is done in order to make a correct transaction and to make the data standard. This can be calculated using the Equation (7). In this way, all data is scaled to the 0-1 value range and the sensitivity is increased.

$$D = \sqrt{\sum_{i=1}^{k} \left(x_i - y_i \right)^2} \tag{4}$$

$$D = \sum_{i=1}^{k} | x_i - y_i | \tag{5}$$

$$D = \left(\sum_{i=1}^{k} \left(| x_i - y_i | \right)^q \right)^{\frac{1}{q}} \tag{6}$$

$$X_{norm} = \frac{X - X_{\min}}{X_{\max} - X_{\min}} \tag{7}$$

3.3 Support vektor machines algorithm and results

A support vector machine (SVM) creates n - dimensional hyperplane that optimally divides the data into two categories. SVM model uses a sigmoid kernel function which has a two-layer feed forward neural network [29-32]. SVM is a statistical learning method that minimizes the square of the average error between the model and the data set. One of the main assumptions of SVM is that all the examples in the training set are independent and similarly distributed. The fractal dimensions of each subject whose image was taken from -30º to 30º intervals were calculated in 5º intervals in order to identify the individuals by calculating the fractal dimensions from the image. In this way a database was created containing different subjects. Fractal dimension values of some of these people are given in Table 2 according to the angles.

Table 2. Fractal dimensions of the subjects at 5 degree intervals

Subject	-30º	-25º	-20º	15º	10º	5º	0º
1	1.97011329498869	1.96722757801438	1.97033911980933	1.97160605503350	1.97239256129616	1.97294658984929	1.97205146902002
2	1.97635260465463	1.97709505800236	1.97870163661989	1.97918620465923	1.97859385993415	1.97907906988785	1.98071515123288
3	1.98071515123288	1.97970620860094	1.98031075691879	1.97806199717433	1.97720135706369	1.97694832130996	1.97765075021474
4	1.97337836036329	1.97276609495383	1.97257089683571	1.97369962444532	1.97170364186763	1.97396532450564	1.97550764013372
5	1.96203455669760	1.96468400003007	1.96019683021413	1.96190544707840	1.96282006686978	1.96123483956897	1.96258980976735
6	1.97644101884035	1.97518667081443	1.97453498154157	1.97414107772730	1.97391799910001	1.97442995353509	1.97632220784728
7	1.97947638967483	1.97969841816441	1.98021128779499	1.98021355600610	1.98061346624025	1.98095233929755	1.98226717870651
8	1.97431217905426	1.97428865845404	1.97458155057724	1.97313671701552	1.97583102312823	1.97581261848193	1.97616681436601

Subject	0º	5º	10º	15º	20º	25º	30º
1	1.97205146902002	1.97352543267791	1.97204151237992	1.97202744601351	1.97203142256673	1.97064334841200	1.97031196697373
2	1.98071515123288	1.97970620860094	1.98031075691879	1.97806199717433	1.97720135706369	1.97694832130996	1.97765075021474
3	1.97554059759455	1.97479944587486	1.97377799422695	1.97220270160952	1.97508616213172	1.97243515631079	1.97319901350586
4	1.97550764013372	1.97354698539303	1.97091402783307	1.97168776213703	1.97197206560398	1.97077802884143	1.97110449641902
5	1.96258980976735	1.96132640276818	1.96172692738985	1.96028152163900	1.96242837747740	1.95992694363105	1.96147251090124
6	1.97632220784728	1.97611713752464	1.97463034508597	1.97659266541862	1.97525735897282	1.97336424843789	1.97375672457208
7	1.98226717870651	1.98039646533888	1.98174017816529	1.98086856357890	1.97895486333172	1.98035685736426	1.97958357187883
8	1.97466314800278	1.97563701265256	1.97542129916197	1.97542977294044	1.97377365652362	1.97466314800278	1.97563701265256

The data used for the Knn algorithm consists of fractal dimension values at 8th iteration that were previously extracted from the hand vein images. However, a technique called shift register is used to increase the recognition of the image that can come from a different angle. The data received here has been shifted within itself and created more than once for the data belonging to the subject in Table 3. In this way, when the image of the subject comes at a different angle, the image closest to that image can be selected in database.

Table 3. Shifted dataset fractal dimensions of the subjects

Number of data	Subject	Rotation Angle (x)													
1	1	-30º	**1.970 312**	1.970 113	1.967 228	1.970 339	1.971 606	1.972 393	1.972 947	1.972 051	1.973 525	1.972 042	1.972 027	1.972 031	1.970 643
2		-25º	1.970 643	**1.970 312**	1.970 113	1.967 228	1.970 339	1.971 606	1.972 393	1.972 947	1.972 051	1.973 525	1.972 042	1.972 027	1.972 031
3		-20º	1.972 031	1.970 643	**1.970 312**	1.970 113	1.967 228	1.970 339	1.971 606	1.972 393	1.972 947	1.972 051	1.973 525	1.972 042	1.972 027
4		-15º	1.972 027	1.972 031	1.970 643	**1.970 312**	1.970 113	1.967 228	1.970 339	1.971 606	1.972 393	1.972 947	1.972 051	1.973 525	1.972 042
5		-10º	1.972 042	1.972 027	1.972 031	1.970 643	**1.970 312**	1.970 113	1.967 228	1.970 339	1.971 606	1.972 393	1.972 947	1.972 051	1.973 525
6		-5º	1.973 525	1.972 042	1.972 027	1.972 031	1.970 643	**1.970 312**	1.970 113	1.967 228	1.970 339	1.971 606	1.972 393	1.972 947	1.972 051
7		0º	1.972 051	1.973 525	1.972 042	1.972 027	1.972 031	1.970 643	**1.970 312**	1.970 113	1.967 228	1.970 339	1.971 606	1.972 393	1.972 947
8		5º	1.972 947	1.972 051	1.973 525	1.972 042	1.972 027	1.972 031	1.970 643	**1.970 312**	1.970 113	1.967 228	1.970 339	1.971 606	1.972 393
9		10º	1.972 393	1.972 947	1.972 051	1.973 525	1.972 042	1.972 027	1.972 031	1.970 643	**1.970 312**	1.970 113	1.967 228	1.970 339	1.971 606
10		15º	1.971 606	1.972 393	1.972 947	1.972 051	1.973 525	1.972 042	1.972 027	1.972 031	1.970 643	**1.970 312**	1.970 113	1.967 228	1.970 339
11		20º	1.970 339	1.971 606	1.972 393	1.972 947	1.972 051	1.973 525	1.972 042	1.972 027	1.972 031	1.970 643	**1.970 312**	1.970 113	1.967 228
12		25º	1.967 228	1.970 339	1.971 606	1.972 393	1.972 947	1.972 051	1.973 525	1.972 042	1.972 027	1.972 031	1.970 643	**1.970 312**	1.970 113
13		30º	1.970 113	1.967 228	1.970 339	1.971 606	1.972 393	1.972 947	1.972 051	1.973 525	1.972 042	1.972 027	1.972 031	1.970 643	**1.970 312**
14	2	-30º	**1.977 651**	1.976 353	1.977 095	1.978 702	1.979 186	1.978 594	1.979 079	1.980 715	1.979 706	1.980 311	1.978 062	1.977 201	1.976 948
15		-25º	1.976 948	**1.977 651**	1.976 353	1.977 095	1.978 702	1.979 186	1.978 594	1.979 079	1.980 715	1.979 706	1.980 311	1.978 062	1.977 201
16		-20º	1.977 201	1.976 948	**1.977 651**	1.976 353	1.977 095	1.978 702	1.979 186	1.978 594	1.979 079	1.980 715	1.979 706	1.980 311	1.978 062
.	.	.	.	.	.	.	.	.	.	.	.	.	.	.	.
129	10	25º	1.974 28865 84540 4	1.974 5815 5057 724	1.973 13671 70155 2	1.975 83102 31282 3	1.975 81261 84819 3	1.976 16681 43660 1	1.975 64384 63315 5	1.974 66314 80027 8	1.975 63701 26525 6	1.975 42129 91619 7	1.975 42977 29404 4	**1.973 77365 65236 2**	1.974 31217 90542 6
919	10	30º	1.974 31217 90542 6	1.974 2886 5845 404	1.974 58155 05772 4	1.973 13671 70155 2	1.975 83102 31282 3	1.975 81261 84819 3	1.976 16681 43660 1	1.975 64384 63315 5	1.974 66314 80027 8	1.975 63701 26525 6	1.975 42129 91619 7	1.975 42977 29404 4	**1.973 77365 65236 2**

In order to test the success of the application, the image of the subject was taken at a different angle and fractal dimensions were calculated. Fractal values were produced by rotating 2 degrees to test the independence of each image produced. In order to test the success of the application, the image of the vein was taken at a different angle and its fractal dimensions were calculated. Fractal values were produced by rotating 2 degrees to test the independence of each image produced. In the output, the subject number is given, stating which image it belongs to in Table 4. The successful ones of the tested values are written as TRUE or FALSE next to the test results. Incorrect values in this data were encountered in the data from the 6th subject. Since the fractal value of the 6th subject was very close to the 8th subject's fractal value, only incorrect results were obtained in this subject. In order to prevent this, it is thought to obtain more accurate results by performing morphological operations on the image taken from the subjects.

Table 4. Test Dataset for fractal dimensions of the subjects

Number of data	Subject	Rotation Angle (x)	-30+x	-25+x	-20+x	-15+x	-10+x	-5+x	0+x	5+x	10+x	15+x	20+x	25+x	30+x	TEST RESULTS
1	1	2°	**1.969 6761 2797 978**	1.969 5722 4354 835	1.969 3059 3776 213	1.971 0563 7093 838	1.972 6024 9162 501	1.973 6846 6484 192	1.972 6732 2651 535	1.972 2690 9626 874	1.972 6317 4599 198	1.972 1631 4934 979	1.970 6734 1936 023	1.970 2288 6275 340	1.970 9729 1383 281	TRUE
2	1	7°	1.970 9729 1383 281	**1.969 6761 2797 978**	1.969 5722 4354 835	1.969 3059 3776 213	1.971 0563 7093 838	1.972 6024 9162 501	1.973 6846 6484 192	1.972 6732 2651 535	1.972 2690 9626 874	1.972 6317 4599 198	1.972 1631 4934 979	1.970 6734 1936 023	1.970 2288 6275 340	TRUE
.	.	.	.	.	.	.	.	.	.	.	.	.	.	.	.	.
14	2	2°	**1.977 3647 2389 813**	1.978 1294 4447 800	1.977 4932 2206 658	1.977 5025 4009 196	1.977 6063 1089 364	1.977 4478 9148 104	1.977 3915 3409 374	1.979 7942 0618 733	1.978 9310 9570 031	1.978 9973 7758 070	1.978 0856 0228 570	1.979 1810 9622 265	1.977 1007 8578 160	TRUE
15	2	7°	1.977 1007 8578 160	**1.977 3647 2389 813**	1.978 1294 4447 800	1.977 4932 2206 658	1.977 5025 4009 196	1.977 6063 1089 364	1.977 4478 9148 104	1.977 3915 3409 374	1.979 7942 0618 733	1.978 9310 9570 031	1.978 9973 7758 070	1.978 0856 0228 570	1.979 1810 9622 265	TRUE
.	.	.	.	.	.	.	.	.	.	.	.	.	.	.	.	.
919	155	7°	1.974 2798 2626 741	1.975 0977 7477 916	1.974 7280 3416 635	1.975 1595 9568 407	1.977 1623 8678 195	1.976 8395 6359 549	1.976 5523 3631 733	1.975 5433 7175 739	1.975 6821 7193 130	1.974 7238 2992 071	1.974 0908 1509 176	1.974 8579 8204 696	1.975 3179 7500 120	TRUE

The k parameter selected in the Knn algorithm significantly affects the result of the operation performed. Since the feature values obtained here are very close to each other, k parameter is chosen as 1. The Knn algorithm and SVM used in this study has 13 inputs and 1 output value. Using fractal dimension, those algorithms has been experimented on two different dataset which are SUAS hand vein image database and Bosphorous Database.

Table 5. Accuracy rates of KNN and SVM models

	KNN			SVM		
	K = 1	K = 5	K = 11	Lineer (LKF)	Polinom (PKF)	Radial (RBF)
Experiment1: SUAS Database	87.5%	88.5%	88.5%	100%	97.5%	45%
Experiment2: Bosphorous Database [33]	85.5%	85%	86%	99%	95%	40%

The training data consisting of fractal values at different angles on the image produced for the test were trained with Knn and then tested with the test data. In the transactions performed, 117 correct results were obtained on 130 data. When the recognition process is performed on the image of the vessel with this method, %85-88.5 success was achieved with the knn algorithm but SVM with LKF and LPF gave much better performance. The results are given in Table 5.

3. Conclusion

In this study, identification was made from the images of dorsal hand vein. With the help of the infrared camera, the SUAS database was created with the vein images collected from the subjects. The collected vein images were normalized and target areas of 256x256 pixels were extracted. Vein areas are segmented by applying pre and post image processing techniques on

target regions. Fractal size-based box counting method was used for feature extraction on the images converted into 1 bit. Fractal dimensions of the processed vessel images of each person in databases were calculated at 7 different angles (from -30 to 30 degrees with an interval of 10 degrees). In this way, the fractal dimensions extracted from the images that are resistant to rotation are stored in the database for use in identification. Datasets trained using SVM and Knn algorithms were then tested. As a result of the tests performed on the SUAS database, 100% performance rate was achieved with the SVM classification algorithm.

Declaration of interests

The authors declare that they have no known competing financial interests or personal relationships that could have appeared to influence the work reported in this paper.

Disclosures

The authors declare no conflicts of interest.

Acknowledgments

We would like to thank to Dr. Bulent Sankur for sharing their Bosphorous Database. Also, we would like to thank volunteer participants to create the SUAS Database.

References

[1] Tanaka T., Kubo N., Biometric authentication by hand vein patterns, SICE, Annual Conference in Sapporo, 249-253, August, 2004.

[2] Liu Z.H., YIN J., JIN Z., An adaptive feature and weight selection method based on gabor image for face recognition, Acta Photonica Sin, 40 (4), 636–641, 2011.

[3] Li, Xi, et al. "A Dorsal Hand Vein Pattern Recognition Algorithm." 2010 3rd International Congress on Image and Signal Processing, 2010, doi:10.1109/cisp.2010.5647776.

[4] Wang, L., et al. "Infrared Imaging of Hand Vein Patterns for Biometric Purposes." IET Computer Vision, vol. 1, no. 3, Jan. 2007, pp. 113–122., doi:10.1049/iet-cvi:20070009.

[5] Khan, M. Heenaye-Mamode, et al. "Representation of Hand Dorsal Vein Features Using a Low Dimensional Representation Integrating Cholesky Decomposition." 2009 2nd International Congress on Image and Signal Processing, 2009, doi:10.1109/cisp.2009.5304218.

[6] Lajevardi, Seyed Mehdi, et al. "Hand Vein Authentication Using Biometric Graph Matching." IET Biometrics, vol. 3, no. 4, Jan. 2014, pp. 302–313., doi:10.1049/iet-bmt.2013.0086.

[7] Wang, Yiding, et al. "Personal Identification Based on Multiple Keypoint Sets of Dorsal Hand Vein Images." IET Biometrics, vol. 3, no. 4, Jan. 2014, pp. 234–245., doi:10.1049/iet-bmt.2013.0042.

[8] Huang, Di, et al. “Dorsal Hand Vein Recognition via Hierarchical Combination of Texture and Shape Clues.” Neurocomputing, vol. 214, 2016, pp. 815–828., doi:10.1016/j.neucom.2016.06.057

[9] SUAS (Sakarya University of Applied Sciences) Dorsal Hand Vein Database. (Available Online) DOI: 10.13140/RG.2.2.11019.44321 https://www.researchgate.net/publication/338117068_SUAS_Dorsal_Hand_Vein_Database

[10] M.Z. Yildiz, Ö.F. Boyraz, Development of a low-cost microcomputer based vein imaging system, Infrared Physics & Technology. (2019). Doi:10.1016/j.infrared.2019.02.010.

[11] Bay, H., Ess, A., Tuytelaars, T., Van, G.L., 2008. Speeded-up robust features (SURF). Computer vision and image understanding 110: 346–359.

[12] C. Genç, " Artistic Practices With Fractal Geometry," Master Thesis, Fine Arts Institute, 2019.

[13] C. İlhan, " Fractal Geometry Analysis of Urban Tissue Morphological Change: The Case Study of Bursa, vol. 4, Architecture and Life, no. 1, pp. 117-140, 2019.

[14] N. K. Erdoğan, "Finansal zaman serilerinin fraktal analizi," Aksaray üniversitesi iktisadi ve idari bilimler fakültesi dergisi, vol. 9, no. 4, pp. 49-54, 2017.

[15] C. Brown and L. Liebovitch, Fractal analysis. Sage, 2010.

[16] K. Falconer, Fractal geometry: mathematical foundations and applications. John Wiley & Sons, 2004.

[17] B. Klinkenberg, "A review of methods used to determine the fractal dimension of linear features," Mathematical Geology, vol. 26, no. 1, pp. 23-46, 1994.

[18] M. Kılınç and H. Gözde, "Detection of buried anti-personnel mines in thermal images by circular hough transformation supported active thermography method," Journal of the Faculty of Engineering & Architecture of Gazi University . 2020, Vol. 35 Issue 2, p697-707. 11p.

[19] R. C. Gonzalez, R. E. Woods, and S. L. Eddins, Digital image processing using MATLAB. Pearson Education India, 2004.

[20] Ö. Ediz, " A Generative Approach In Architectural Design Based On Fractals," PhD, Natural of Science Institute, ITU, 2003.

[21] B. Alik, " A Study On Designing Methods And Fractal Coded Designs In Architecture," Master Thesis, Kocaeli University, 2015.

[22] A. O. ÖNCEL, "Fraktal dağılım ve sismolojideki uygulamaları," Jeofizik , vol.9, no.10, pp.311-316, 1995.

[23] S. Pandey, V. Sharma, and G. Agrawal, "Modification of KNN Algorithm," International Journal of Engineering and Computer Science, vol. 8, no. 11, pp. 24869-24877, 2019.

[24] R. O. Duda, P. E. Hart, and D. G. Stork, Pattern classification. John Wiley & Sons, 2012.

[25] S. V. Wawre and S. N. Deshmukh, "Sentiment classification using machine learning techniques," International Journal of Science and Research (IJSR), vol. 5, no. 4, pp. 819-821, 2016.

[26] H. Geppert, M. Vogt, and J. Bajorath, "Current trends in ligand-based virtual screening: molecular representations, data mining methods, new application

areas, and performance evaluation," Journal of chemical information and modeling, vol. 50, no. 2, pp. 205-216, 2010.
[27] M. Al-Maolegi and B. Arkok, "An improved Apriori algorithm for association rules," arXiv preprint arXiv:1403.3948, 2014.
[28] A. Likas, N. Vlassis, and J. J. Verbeek, "The global k-means clustering algorithm," Pattern recognition, vol. 36, no. 2, pp. 451-461, 2003.
[29] Suykens, Johan AK, and Joos Vandewalle. "Least squares support vector machine classifiers." Neural processing letters 9.3 (1999): 293-300.
[30] Cauwenberghs, Gert, and Tomaso Poggio. "Incremental and decremental support vector machine learning." Advances in neural information processing systems. 2001.
[31] Shimodaira, Hiroshi, et al. "Dynamic time-alignment kernel in support vector machine." Advances in neural information processing systems. 2002.
[32] Mangasarian, Olvi. Generalized support vector machines. 1998.
[33] A. Yüksel, L. Akarun, B. Sankur, Biometric Identification Through Hand Vein Patterns, ICPR'2010: Int. Conf. on Pattern Recognition, The First International Workshop on Emerging Techniques and Challenges for Hand-based Biometrics (ETCHB2010), Istanbul, August 2010.